Probing the Phosphates of the *Escherichia coli* Ribosomal 16S RNA in Its Naked Form, in the 30S Subunit, and in the 70S Ribosome†

Florence Baudin, Marylène Mougel, Pascale Romby, Flore Eyermann, Jean-Pierre Ebel, Bernard Ehresmann, and Chantal Ehresmann*

Laboratoire de Biochimie, Institut de Biologie Moléculaire et Cellulaire du CNRS, 15 rue René Descartes, 67084 Strasbourg Cedex, France

Received January 4, 1989; Revised Manuscript Received April 4, 1989

ABSTRACT: Ethylnitrosourea is an alkylating reagent which preferentially modifies phosphates in nucleic acids. It was used to map phosphates in naked *Escherichia coli* 16S rRNA engaged in tertiary interactions through hydrogen bonds or ion coordination. Of the phosphates, 7% are found involved in such interactions, and 57% of them are located in loops or interhelical regions, where they are involved in maintaining local intrinsic structures or long-distance tertiary interactions. The other phosphates (43%) are found in helical regions. These phosphates often occur at the proximity of bulged nucleotides or in irregular helices containing noncanonical base pairs (and bulges) and are assumed to bind cations in order to neutralize negative charges and to stabilize unusual phosphate backbone folding. In the 30S subunit, ENU allowed mapping of phosphates in contact with proteins. The RNA is not uniformly engaged in RNA/protein interactions. Regions 1–51, 250–310, 567–612, 650–670, and 1307–1382 are particularly buried whereas the 3′-terminal domain and the 5′-proximal region (nucleotides 53–218) are exposed. The conformation of 16S rRNA is not drastically affected by protein binding, but conformational adjustments are detected in several defined regions. They are found in the 5′ domain (region 147–172), in the central domain (region 827–872), in the 3′ major domain (nucleotides 955–956, 994, 1054, 1181, 1257, and 1262–1263), and in the 3′-terminal domain (around 1400). The 50S subunit shields clusters of phosphates located at the subunit interface. The most extensive protections are observed in the 3′-terminal domain (1490–1542), in the central region of the molecule (770–930), and in the upper 3′ major domain. The binding of the 50S subunit also causes changes of reactivity in the 3′ part of the central domain (around 830), most likely reflecting dynamic properties in this region.

The use of enzymatic and chemical probes to monitor the conformation of RNAs in solution has been extensively developed in recent years. The combination of probing and sequencing technologies is a sensitive and relevant method to get a detailed insight into the folding of RNA, to study dynamic aspects, and to identify nucleotides in contact with proteins [for a review, see Ehresmann et al. (1987)]. The conformation of *Escherichia coli* 16S rRNA, its folding within the subunit, and its interaction with ribosomal proteins have been investigated by using enzymatic and chemical probing [e.g., see Douthwaite et al. (1983), Moazed et al. (1986), Stern et al. (1986, 1988a,b), Baudin et al. (1987), Mougel et al. (1987, 1988), Svensson et al. (1988), and Powers et al. (1988a,b)] and by RNA/RNA and RNA/protein cross-linking [for a review, see Brimacombe et al. (1988)]. Compilation of available data together with the topographical localization of the 30S proteins (Capel et al., 1987) led to the proposal of three-dimensional structure models of 16S rRNA, which provide a first relative orientation of helices in the subunit (Expert-Bezancon & Wollenzien, 1985; Brimacombe et al., 1988; Stern et al., 1988c). However, any further refinement of these models requires detailed information at the atomic level on the phosphate, ribose, and base moieties. The used chemical reagents modify specific groups of bases, allowing one to get information on Watson–Crick positions and position N7 of purines. Nevertheless, in footprinting experiments, information is generally restricted to unpaired nucleotides. Ethylnitrosourea (ENU)[1] is an *N*-nitroso alkylating reagent which has a high affinity for phosphate group oxygens in nucleic acids (Vlassov et al., 1981). Compared to other chemical probes, ENU shows the advantage not to be selective, since its reactivity is sequence and secondary structure independent. The probing of phosphates with ENU in several RNA species such as tRNAs [e.g., see Vlassov et al. (1981), Garret et al. (1984a), and Romby et al. (1985, 1987)], 5S rRNAs (McDougall & Nazar, 1986; Romby et al., 1988), and turnip yellow mosaic virus tRNA-like structure (Florentz et al., 1982) has revealed specific features of tertiary structure. ENU has also been successfully used to map phosphates in close contact with proteins in various RNA–protein complexes such as aminoacyl-tRNA synthetase/tRNA [e.g., see Vlassov et al. (1983), Garret et al. (1984a), and Romby et al. (1985)] yeast valyl-tRNA synthetase/turnip yellow mosaic virus tRNA-like structure (Florentz & Giegé, 1986), and *E. coli* ribosomal protein S8/16S rRNA (Mougel et al., 1987). ENU can also detect conformational adjustments in RNA induced by protein binding, as shown for tRNA interacting with elongation factor Tu or reverse transcriptase (Riehl et al., 1983; Garret et al., 1984b).

In the present work, we have monitored the reactivity of every phosphate toward ENU in the naked 16S rRNA and followed the reactivity changes induced by 30S subunit assembly and by the binding of the 50S particle. The results are discussed in terms of tertiary folding, RNA/protein to-

† This work was supported by grants from the Centre National de la Recherche Scientifique (CNRS) and the Ministère de la Recherche et de la Technologie (MRT).

* To whom correspondence should be addressed.

[1] Abbreviation: ENU, ethylnitrosourea.

0006-2960/89/0428-5847$01.50/0

pography, conformational adjustments, and the subunit interface.

Experimental Procedures

Buffers. Buffer I: 20 mM Tris-HCl, pH 7.5, 60 mM NH_4Cl, 6 mM magnesium acetate, and 6 mM 2-mercaptoethanol. Buffer II: 20 mM Tris-HCl, pH 7.5, 10 mM magnesium acetate, 60 mM NH_4Cl, 400 mM NaCl, and 6 mM 2-mercaptoethanol. Buffer III: 10 mM Tris-HCl, pH 7.5, 100 mM LiCl, 1 mM EDTA, and 0.5% SDS. Buffer IV: 50 mM sodium cacodylate, pH 7.5, 20 mM magnesium acetate, 300 mM KCl, and 6 mM 2-mercaptoethanol. Buffer V:50 mM sodium cacodylate, pH 7.5, and 1 mM EDTA.

Chemicals and Enzymes. ENU was from Sigma; [5′-^{32}P]pCp (3000 Ci/mmol), [γ-^{32}P]ATP (3200 Ci/mmol), and T_4 polynucleotide kinase were from Amersham; acrylamide and *N,N′*-methylenebis(acrylamide) were from BDH Chemicals; T_4 RNA ligase was from P-L Biochemicals; avian myeloblastosis virus reverse transcriptase was from Life Science.

Preparation of Ribosomal Components. Ribosomal particles and 16S rRNA from *Escherichia coli* were prepared according to Baudin et al. (1987). 70S tight couples were isolated on a 10–30% linear sucrose gradient in buffer I, and 30S subunits were obtained by dissociation of 70S ribosomes through sucrose gradient centrifugation in buffer II. Naked 16S rRNA was obtained by deproteinization of 30S subunits through a 5–25% sucrose gradient in buffer III. The ribosomal components were stored in small samples at −80 °C. They were renatured by incubation at 40 °C for 20 min in buffer IV and cooled on ice prior to alkylation.

Labeling of Ribosomal Components. Labeling of 16S rRNA was achieved within the 30S subunit by using [5′-^{32}P]pCp and T_4 RNA ligase according to England and Uhlenbeck (1978). After precipitation with 0.7 volume of ethanol at 4 °C for 30 min, the labeled 30S subunits were renatured as above and incubated with a 3–5 molar excess of renatured 50S subunits in buffer I at 37 °C for 30 min. Labeled reassociated 70S tight couples were isolated as described above. These labeled 70S ribosomes were used as a source of labeled 30S subunits and 16S rRNA.

Alkylation of 16S rRNA by ENU. Phosphate alkylation was essentially as described by Vlassov et al. (1981). A standard assay contained 12.5 pmol of unlabeled 16S rRNA, 30S subunits, or 70S ribosomes in 20 μL of buffer IV. Incubation was at 37 °C with 5 μL of an ENU-saturated ethanol solution for 30, 60, and 90 min (16S rRNA and 30S subunits) or for 1, 2, and 3 h (for 70S ribosomes). An incubation control was done for each incubation time. Under denaturing conditions, naked 16S rRNA was incubated in buffer V for 15 and 30 s at 90 °C. When 3′ end-labeled RNA was used, 12 μg of tRNA was added as carrier. The reaction was stopped by ethanol precipitation. After phenol extraction, the alkylated RNA was cleaved at phosphotriester positions by incubation in 0.1 M Tris-HCl, pH 9.0, at 50 °C for 15 min. The generated RNA fragments were then ethanol-precipitated and washed.

Detection and Analysis of Alkylated Positions. Cleavage positions were detected by the primer extension method using reverse transcriptase, as described by Mougel et al. (1987) and Baudin et al. (1987). Thirteen oligodeoxyribonucleotides, complementary to nucleotides 110–124, 220–234, 330–344, 440–454, 550–564, 660–674, 761–777, 865–879, 986–1000, 1101–1116, 1220–1240, 1330–1344, and 1435–1449, were synthesized with an Applied Biosystem apparatus. These oligomers were labeled at their 5′ end with [γ-^{32}P]ATP and T_4 polynucleotide kinase according to Silberklang et al. (1977) and were used as primer for reverse transcription. The generated DNA fragments were sized at nucleotide resolution by electrophoresis on 9.5% acrylamide/0.5% bis(acrylamide)/8 M urea slab gels (40 × 30 × 0.04 cm) at 1500 V, for 2 or 4 h. Dideoxy sequencing reactions were made in parallel on unmodified RNA as described by Sanger et al. (1977). The 3′-terminal part of the RNA (nucletodies 1430–1542) was probed by using 3′ end-labeled 16S rRNA, and the resulting RNA fragments were sized by gel electrophoresis. Cleavage positions were identified by running in parallel RNases T_1 and U_2 and formamide ladders.

Results

Experimental Strategy. In this work, we have used ENU to probe the phosphates of 16S rRNA in its naked form, in order to detect phosphates engaged through hydrogen bonding in tertiary interactions or in ion coordination. Phosphates shielded by the proteins within the 30S subunit were mapped as well as possible conformational adjustments induced by protein binding. Lastly, the association of both subunits into 70S ribosomes was investigated, allowing us to map interface regions and again possible rearrangements. Alkylation was achieved under native conditions, and the resulting phosphotriester bonds were cleaved by alkaline treatment. Cleavage positions were localized by the primer extension method for the largest part of the molecule (1–1436), using 13 different primers. The 3′-terminal region (1430–1542) was monitored by using 3′-labeled 16S rRNA. This approach was preferred to the primer extension method because of the presence of two 2,6-dimethyladenines at positions 1518–1519 and of a 2-methylguanine at position 1516 which block the progress of reverse transcriptase. The relative reactivity of phosphates was estimated by visual inspection, taking the reactivity of naked 16S rRNA phosphates alkylated under denaturing conditions (in the absence of magnesium, at 90 °C) as a reference. Under those denaturing conditions, all phosphates are expected to be reactive. The degree of "protection" of phosphates was evaluated as "strong" (more than 50%) or "weak" (less than 50%). It is generally assumed that there is a direct correlation between chemical reactivity and accessibility. This is not necessarily true since chemical reactivity is largely influenced by the electrostatic environment of the atoms. However, theoretical calculations combining steric and electrostatic factors (computation of ASIF or "Accessible Surface Integrated Field") emphasize the existence of a high electrostatic potential around phosphate groups, which implies that the reactivity with electrophilic species is mainly governed by geometrical factors (Lavery & Pullman, 1984). Indeed, a very good corelation was found between the calculated ASIF indexes and the ENU reactivity of phosphates in yeast $tRNA^{Phe}$ (Vlassov et al., 1981) and yeast $tRNA^{Asp}$ (Romby et al., 1985).

Two representative autoradiograms are shown in Figure 1, and the results are summarized in Figure 2 for naked 16S rRNA and 30S subunit and in Figure 3 for 70S ribosome. Information could be obtained on about 92% of the phosphates of the molecule. As for the remaining phosphates, a correct estimation cannot be given because of stops or pauses of reverse transcriptase. Some of these stops result from posttranscriptional methylation of certain residues (see the stop at position 967 corresponding to m^2G, Figure 1A) or to proton-catalyzed hydrolysis, most often occurring at the pyrimidine–adenine phosphodiester bond and reflecting an intrinsic fragility of the molecule (Dock-Bregeon & Moras, 1987). Some of the stops

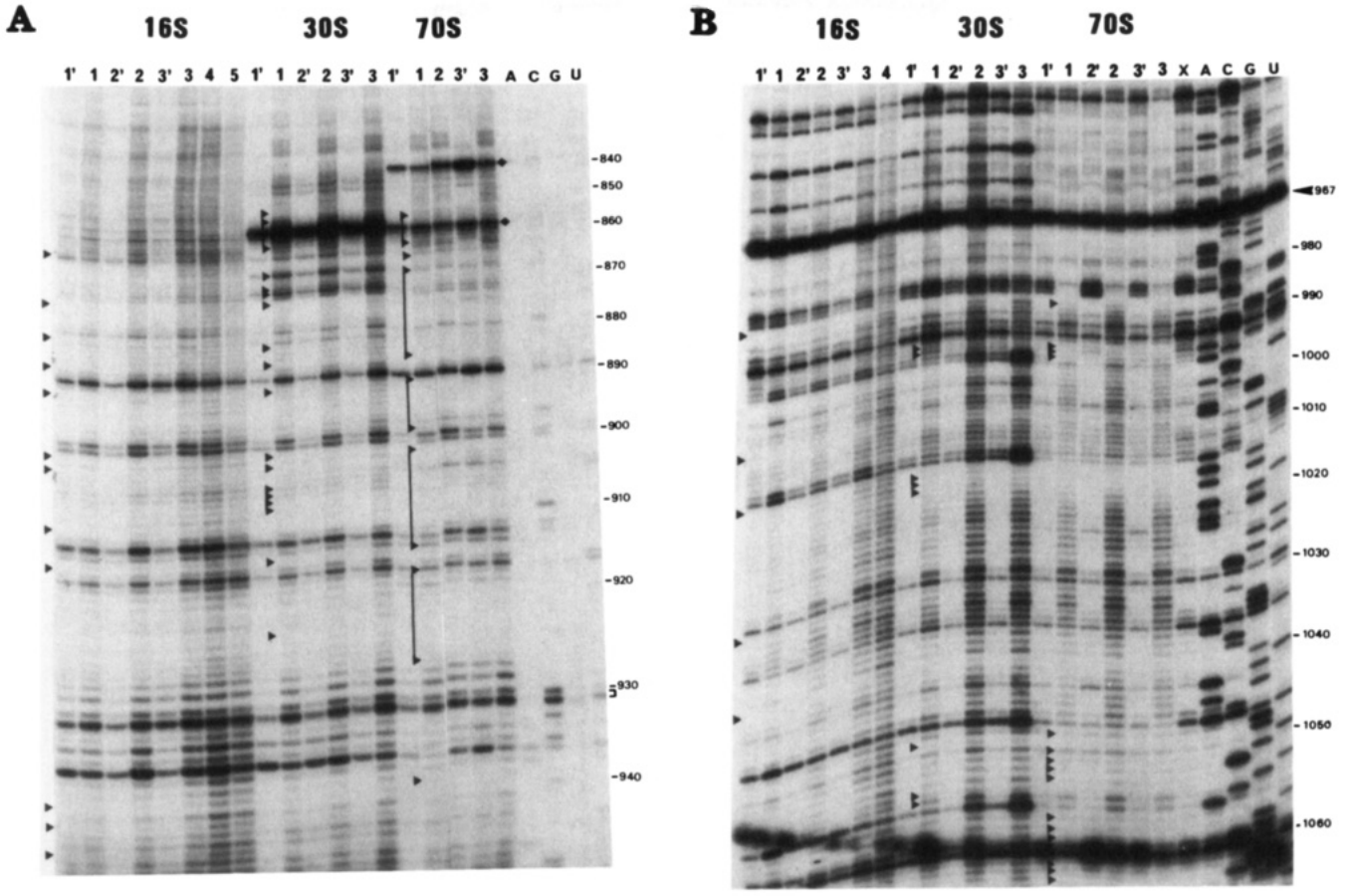

FIGURE 1: Gel electrophoresis fractionation of products resulting from ENU alkylation of naked 16S rRNA, 30S subunits, and 70S ribosomes as monitored by primer extension using (A) the primer 986–1000 and (B) 1101–1116. Alkylation was as described under Experimental Procedures. Incubation was for (1) 30 min, (2) 60 min, and (3) 90 min for 16S rRNA and 30S subunits and for (1) 1 h, (2) 2 h, and (3) 3 h for 70S ribosomes, under native conditions. Lanes 1′, 2′, and 3′ are the respective incubation controls; denaturing conditions: (4) 15 s, (5) 30 s. Arrowheads point to reactivity changes; brackets denote band compression. Lanes A, G, C, and U are sequencing products generated in the presence of ddTTP, ddCTP, ddGTP, and ddATP, respectively.

do not correspond to one of these two cases and may reflect the difficulty for reverse transcriptase to melt particularly stable regions.

Naked 16S rRNA. About 7% of the phosphates (i.e., 110) have a decreased reactivity in the native RNA as compared to the denatured RNA (Figure 2). Among them, 38 phosphates show a strong protection. The protected phosphates are found spread out in the entire molecule, with a higher density in a complex branched structure in the 5′ domain (nucleotides 144–221) and in an irregular stem–loop structure in the central domain (nucleotides 590–650). Of the protected phosphates, 57% (i.e., 64) are found in loops and interhelical or hinge regions. Among the 46 phosphates protected in helical regions, 25 are located in irregular portions of helices containing bulges and/or noncanonical base pairs (U-G, A-G, U-U) or in their close proximity. The most striking example concerns helix 592–599/639–647. This region, which binds ribosomal protein S8, has been fully described elsewhere (Mougel et al., 1987) and has been proposed to contain one noncanonical base pair involving U_{598} and U_{641} and three bulged adenines at positions 595, 640, and 642. However, protection is not systematically observed in such irregular regions. The other 21 protected phosphates are located in regular helices, but it might be relevant that 16 of them appear to be engaged in the phosphodiester bond linking the two base pairs which close external or internal loops (e.g., P_{37}, P_{613}).

16S rRNA within the 30S Subunit. The binding of the 21 ribosomal proteins induces the protection of a relatively low number of phosphates (17% of the phosphates) (Figure 2). Strikingly, up to 76% of the RNA appears to still be accessible to ENU. Twenty-one phosphates which are partially protected in naked RNA show an increased protection. The additional protections are not evenly distributed along the molecule. The highest densities of protected phosphates are observed in regions 1–51, 250–310, 567–612, 650–670, and 1307–1382, while some other regions such as the 3′-terminal domain and the 5′-proximal region (positions 53–218) show a quasi-absence of protection. Beside protection, the binding of proteins also caused an enhanced reactivity of 28 phosphates. The most pronounced effect occurs in the 5′ domain (region 147–151) and in the central domain (region 827–872) (see Figure 1A) where clusters of phosphate become even more reactive than in the denatured RNA. Note that another class of phosphates, being protected in naked 16S rRNA (positions 170, 172, 891, 1181, and 1401), becomes fully reactive in the 30S subunit. Another consequence of subunit assembly is the increased level of reverse transcriptase stop at positions 240 and 857 (see Figure 1A).

16S rRNA within the 70S Ribosome. The protections induced by the association of the two subunits are clustered in defined RNA regions: mainly the 3′- proximal part (region 1410–1542), the upper 3′ major domain (region 960–1220), and the 3′ part of the central domain (region 855–930) (Figure 3). More limited protections also occur in the central domain (regions 622–627, 663–710, and 770–786). On the other hand, the 5′ domain is only weakly affected: some of the protections already observed in the isolated 30S subunit (phosphates 9–10, 20–21, 46, and 357) are increased in the 70S ribosome, and

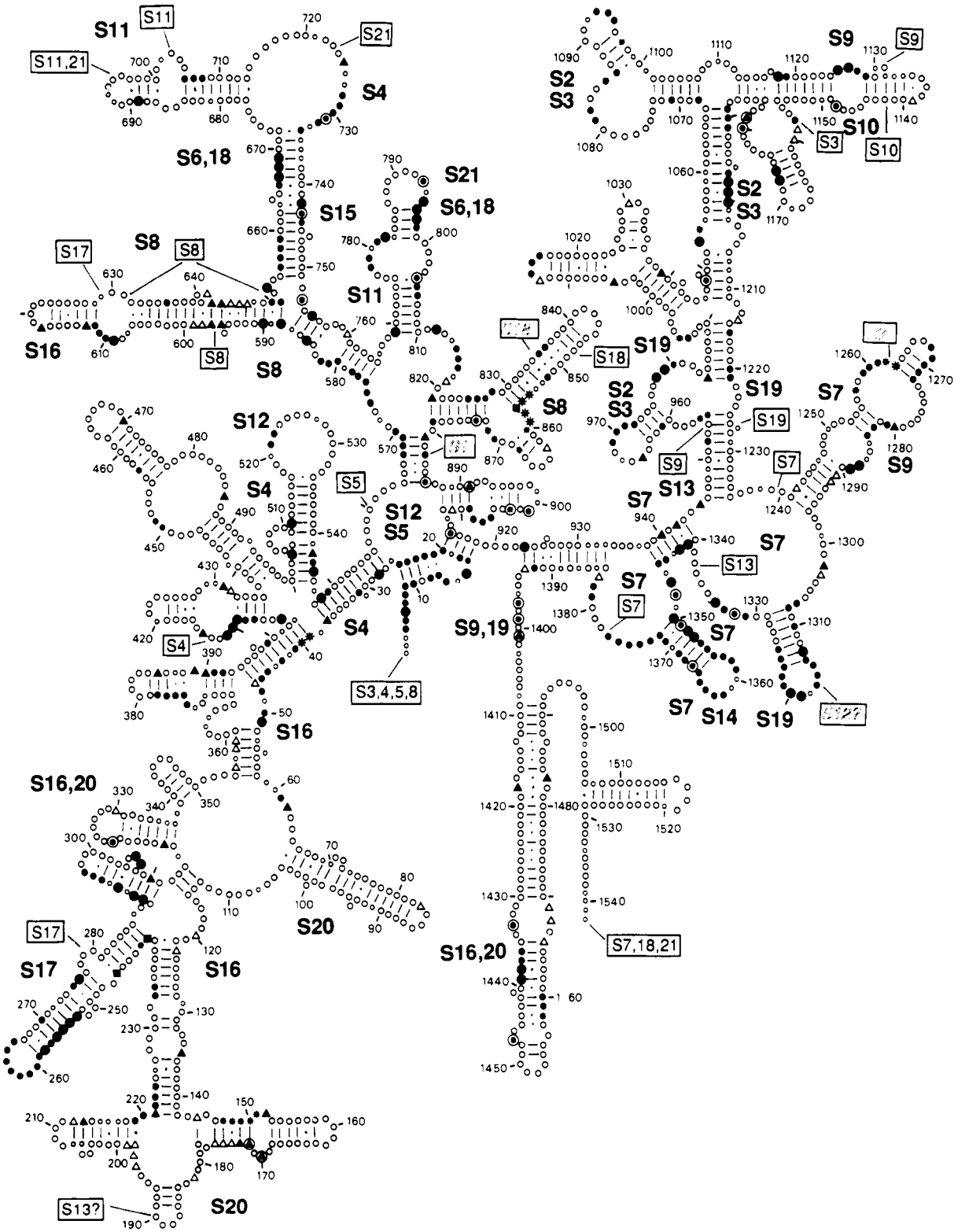

FIGURE 2: Schematic diagram of the 16S rRNA secondary structure showing the position of phosphates protected from ENU alkylation in naked RNA and in the 30S subunit. The secondary structure model is from Moazed et al. (1986) with modifications in region 641–642 according to Mougel et al. (1987) and in region 1073–1085 and helix 1046–1067/1189–1221 according to Baudin et al. (1987). Canonical base pairs are represented by bars and noncanonical base pairs (U·G, A·G, or U·U) by dots. The reactivity of phosphates is summarized as follows: (△, ▲) weakly or strongly protected in both naked 16S rRNA and 30S subunit; (⊙) weakly protected in naked RNA and strongly protected in 30S subunit; (◬) protected in naked RNA but not in 30S subunit; (•, ●) reactive in naked 16S rRNA and weakly or strongly protected in 30S subunit; (small star, large star) reactive in 16S rRNA and weakly or strongly enhanced in 30S subunit; (◦) undetermined, due to stop of reverse transcriptase; (♦) increased stop of reverse transcriptase in 30S subunit. This figure also summarized the location of RNA–protein cross-linking sites, with cross-linked proteins enboxed. References are from Ehresmann et al., (1980) for S7, Golinska et al. (1981) for S1, Moine et al. (1988) for S18, Chiaruttini et al. (1982) for S12, and Brimacombe et al. (1988) for all other proteins. Note that the cross-linking site of S12 could not be found again, using another identification technique (Chiaruttini et al., 1986), and cannot easily be fitted with the position of S12 in the 30S subunit as determined from neutron scattering (Capel et al., 1987). The main regions found protected by proteins are also indicated by boldface capitals; the results are from Stern et al. (1986, 1988a,b) for S4, S5, S11, S12, S16, S17, S20, and S21, from Svensson et al. (1988) for S6, S8, S15, and S18, from Mougel et al. (1987, 1988) for S8 and S15; and from Powers et al. (1988a,b) for S2, S3, S7, S9, S10, S13, S14, and S19.

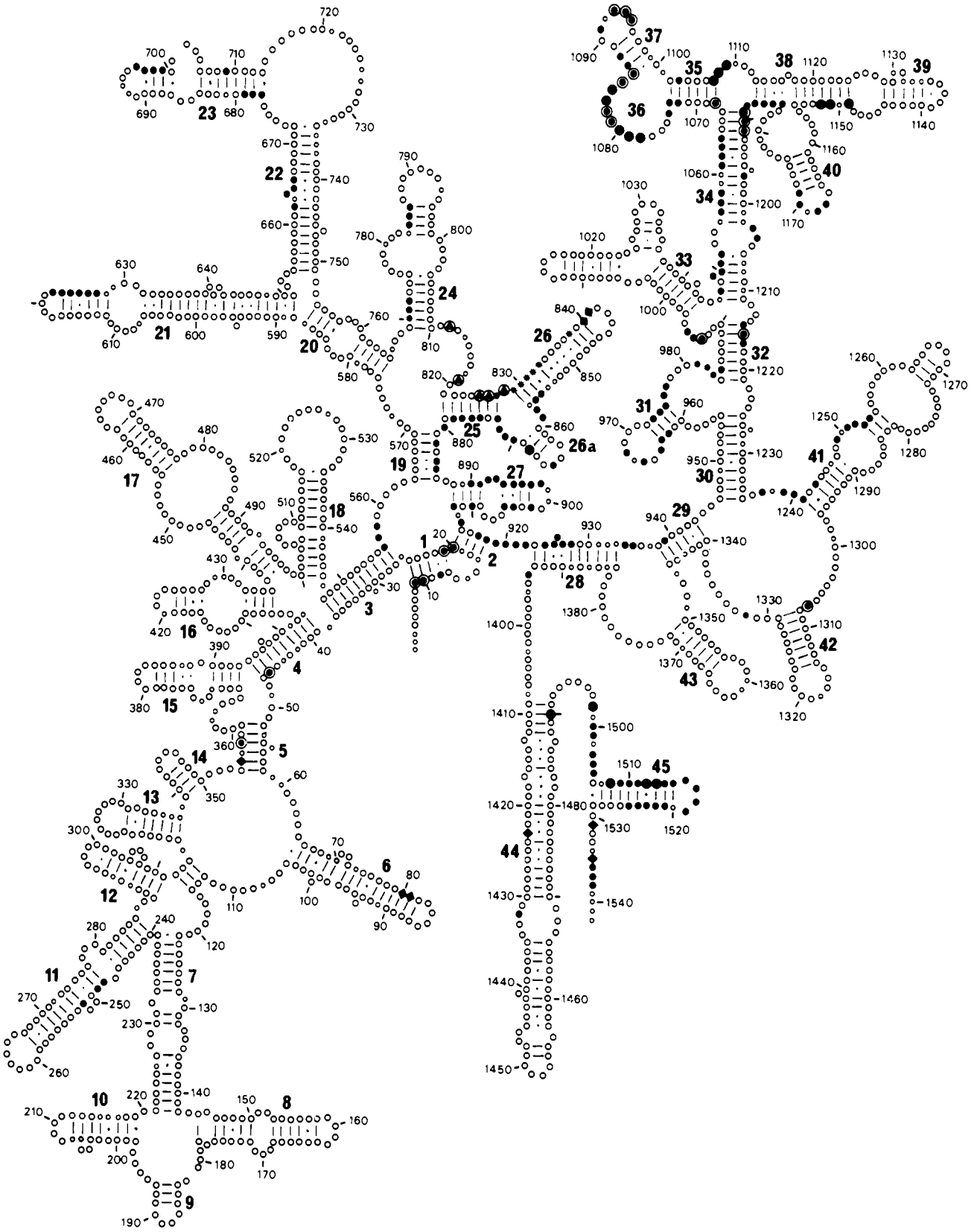

FIGURE 3: Comparison of the reactivity of 16S rRNA phosphates in the 70S ribosome relative to the 30S subunit. Same symbols as in Figure 2. Helices are numbered according to Brimacombe et al. (1988). Only the reactivity changes induced by 50S subunit association are given.

new protections are induced at phosphates 247–248 and 252. Furthermore, the subunit association induces an enhanced reactivity at several phosphates. This effect is restricted to a defined RNA region in the central domain (region 812–838). Two classes of enhancements can be distinguished. The first one (phosphates 812, 819, 825–826, and 828) is protected in the 30S subunit and does not show any significant protection in the 70S ribosome, while the second one (phosphates 829–833) is already reactive in the isolated subunit. Note also that phosphates 855–856 and 858–859, which have an enhanced reactivity in the subunit as compared to naked RNA, regain the same level of reactivity in the 70S ribosome as in the naked RNA. Remarkably, new stops of reverse transcription are induced in the same area (at positions 840–841),

in the 5′ domain (at positions 80–81 and 355), and in the 3′-terminal domain (at positions 1423, 1531, and 1535).

Discussion

Structural Implications in 16S rRNA. We found that 7% of the phosphates are protected from ENU alkylation in naked 16S rRNA. This represents a good approximation since 92% of the total phosphates could be tested with accuracy. Rather unexpectedly, the prevailing localization of protected phosphates is not in single-stranded regions. As a matter of fact, protected phosphates are found in loops or interhelical regions but also in helical regions. This is rather surprising since phosphates in helices are external and fully exposed. In order to understand the cause of the observed protections, a comparison can be made with the well-documented case of tRNAs in which a correlation could be made between the crystal structure and the ENU reactivity in solution. In the tRNAs studied so far, it was evident that all protected phosphates form tertiary interactions through hydrogen bond with other groups of the molecule or are coordinated with magnesium ions (Vlassov et al., 1981; Romby et al., 1985). The tertiary interactions may stabilize intrinsic conformations such as the T loop, in which phosphate 60 forms hydrogen bond with position N4 of C_{61} and the 2′-OH of ribose 58 (Jack et al., 1977; Quigley et al., 1978; Westhof et al., 1985; Romby et al., 1987). The tertiary interactions can also involve groups located in distant part of the molecule, thus participating in the tertiary folding of the molecule (e.g., the interaction of phosphate 22 in the D loop of $tRNA^{Asp}$ with the N6 atom of A_{46} in the variable loop). In 16S rRNA, it is obviously difficult to discriminate between phosphates engaged in local or long-range interactions. However, in the particular case of phosphate 618, a long-distance interaction can be postulated since the protection of phosphate 618 was found to occur in the complete 16S rRNA but not in an RNA fragment covering nucleotides 578–756 (Mougel et al., 1987). Note that nucleotides 618–626 and 1420–1426 were cross-linked with psoralen in the 16S rRNA, suggesting a close vicinty of these two regions (Thompson & Hearst, 1983). Protection may also be related to magnesium coordination. Such a correlation was done in the case of both $tRNA^{Phe}$ and $tRNA^{Asp}$, in which phosphates 8–11 are coordinated to a magnesium ion (Jack et al., 1977; Quigley et al., 1978; Westhof et al., 1985).

In 16S rRNA, protected phosphates are frequently found in irregular helical regions near bulges or noncanonical base pairs. Ion binding may account for the observed protections, since cations might be necessary for neutralizing negative charges of phosphates and maintaining the unusual phosphate backbone folding. In 5S rRNAs, protected phosphates have also been found in an irregular helical region (Romby et al., 1988; Romaniuk et al., 1988). In the latter cases as well as in the case of the 16S rRNA irregular helix 592–599/639–647 (Mougel et al., 1987), magnesium is required for maintaining these particular conformations, suggesting that protected phosphates located in noncanonical helices may represent privileged binding sites for magnesium. The protection of phosphates located in regular helices is more difficult to understand. The fact that they are mostly located at one extremity of helices may be significant, possibly reflecting some intrinsic structure. Nevertheless, they might also be engaged in long-range tertiary interactions, as observed for phosphate 23 in the D stem of yeast $tRNA^{Phe}$, which forms a hydrogen bond with position N6 of A_9 (Holbrook et al., 1978). It must be mentioned that some of the protections observed either in paired or in unpaired regions might also result from some steric hindrance linked to particular tertiary folding.

Recently, a new pseudoknot-type structure has been postulated in region 821–879 (Stern et al., 1988c). In this model, the two base pair 861–862/867–868 helix is stacked between helix 821–827/873–879 and a tertiary 570–571/865–866 interaction. This pseudoknot-type requires single strands to cross helix grooves. Therefore, the protection of phosphates 821, 863, and 874 may fit with such a model, and it can be imagined that these phosphates are involved in this structure through hydrogen bonding. Also, the protection of phosphate 881 in the neighboring helix may be related to this particular spatial arrangement.

Effect of 30S Subunit Assembly. As a first consequence of the binding of ribosomal proteins, most of the phosphates which are found protected in the naked RNA are also protected in the subunit. This indicates that the conformation of 16S rRNA is not drastically perturbed by the 30S subunit assembly. However, a loss of protection is observed at five positions (170, 172, 891, 1181, and 1401) which most likely indicates a local conformational adjustment. Besides, the protection of several phosphates is found reinforced in the subunit. This can be interpreted either (i) as a shielding effect caused by a bound protein near the concerned phosphate or (ii) as a protein-induced stabilization of a particular conformation. Some of these protected phosphates (731, 743, 804, 1332, 1348, 1351, 1367) are located in clusters of newly protected phosphates and most likely correspond to the first class. The other phosphates (170, 172, 874, 1180, 1397, 1399) are isolated and located near positions where enhanced reactivities are observed; they probably correspond to the second class. The new protections observed in the subunit as compared to the naked RNA represent the footprints of the various ribosomal proteins. The small size of the probe allows us to attack nonprotected phosphates near the protein, thus accounting for the rather high proportion of phosphates which are still reactive in the subunit. Two types of protection can be observed: isolated protection, probably reflecting point contacts with proteins, and cluster of protected phosphates, resulting from shielding effects. There is a nice correlation with the present observations and other experimental data obtained by cross-linking and footprinting experiments. These results are summarized in Figure 3, allowing an easy comparison. The lower half of the 3′ major domain appears to be extensively involved in protein binding. For instance, multiple sites have been evidenced for proteins S7, S9, and S19 (Powers et al., 1988a). Note that the S8-induced protection of phosphates 590, 636, 650, and 651 observed in the S8–16S rRNA complex (Mougel et al., 1987) is also observed in the complete subunit. Remarkably, the 3′-terminal domain has very little contact with proteins (with the exception of S16 and S20). Proteins S7, S18, and S21 which have been cross-linked to the 3′ extremity should be in close proximity of this part of the RNA, but do not likely interact with this region.

The enhanced reactivities most likely reflect local conformational adjustments. Nevertheless, it cannot be excluded that some of the isolated protections may also result from such an effect. Remarkably, enhanced reactivities are most often observed in or near regions which have been shown to be in contact with proteins (see Figure 2). It should be noted that the protein-induced adjustments detected by the use of other chemical probes are not all revealed by ENU probing. In particular, the rearrangement observed at residues 1063–1064 and 1192 (Baudin et al., 1987), probably forming the spectinomycin binding site (Sigmund et al., 1984; Moazed & Noller, 1987), does not cause an enhanced reactivity toward

ENU. The conformational adjustments occurring in regions around residues 1400 and 1260 are detected by both base- and phosphate-specific probes. An enhanced reactivity is also observed at phosphate 1054, located in a region facing A1201 which has been shown to display an enhanced reactivity as a result of 30S assembly (Baudin et al., 1987) and more precisely of the polyspecific effect of S2, S3, S10, and S14 binding (Powers et al., 1988b). Otherwise, other structural changes are revealed by ENU, especially in the 827–872 region. Binding of proteins also causes the appearance of new very strong stops of elongation (at positions 240, 245, and 857). These stops can probably be interpreted as the result of spontaneous cleavages reflecting an increased flexibility of the RNA backbone induced by protein binding. Strikingly, the increased cleavage at position 857 occurs in a "hot" region where enhanced reactivities are observed. It is relevant that structural adjustments are observed in two functionally strategic regions: the 1400 region involved in the decoding process (Ofengand et al., 1986) and region 827–891 probably involved in the transitional initiation since protein S1 (Golinska et al., 1981), protein S18 (Greuer et al., 1987; Moine et al., 1988), and initiation factor III (Ehresmann et al., 1986) have been cross-linked in this area. This emphasizes the role of ribosomal protein in building the ribosomal functional sites.

Effect of Ribosome Association. The additional protections observed in the presence of the large subunit are restricted to defined RNA regions and most often affect clusters of phosphates (Figure 3). This is not surprising since the shielding effect induced by the 50S subunit is expected to be important and not only limited to isolated contacts. The observed protections delimit the face of the 30S subunit located at the interface and provide detailed topographic information on the 16S rRNA portions which are exposed on this particular face of the subunit. Some information on the reactivity of bases and on the accessibility to enzymes is also available from earlier studies (Chapman & Noller, 1977; Herr et al., 1979; Vassilenko et al., 1981; Baudin et al., 1987). However, they are rather limited, due to the nature of the probes used: only a few bases are reactive in the 30S subunit, and enzymes suffer from steric hindrance effects. In fact, a satisfying general agreement is obtained between these results and ENU probing. In particular, the protections from kethoxal are restricted in the central domain (G674, G703, G705, G791, G818), in the 3′ major domain (upper part: G1094, G1098, G1166), and in the 3′-terminal domain (G1405, G1497, G1516–1517) (Chapman & Noller, 1977; Herr et al., 1979). This also fits with protections seen with RNase V_1 in the central domain (position 773) and in the 3′-terminal domain (positions 1389, 1408, 1409, 1439, and 1440) (Vassilenko et al., 1981). It should be noted that the protection of position 337, the only site protected from RNase V_1 in the 5′ domain, cannot be directly correlated with phosphate protection. Mapping experiments of the 3′ major domain confirm the localization of the upper part near the interface (Baudin et al., 1987). However, results regarding helix 1046–1067/1189–1211 are equivocal. Guanines 1190, 1193, 1198 are clearly protected from dimethyl sulfate at N7, C1203 at N3 and A1204 at N1, as a result of 50S association. Besides, several nucleotides (C1063, G1064, C1192, and A1201) which already show an enhanced reactivity induced by protein assembly are still highly reactive and even display a further enhancement of reactivity (especially in the case of A1201). These observations are also corroborated by the finding that G1053, G1064, and G1068 were also found more reactive to kethoxal in the 70S ribosome (Herr et al., 1979). However, only protections are observed with ENU in this helix as the result of 50S binding. It should be noted that the reactivity of phosphate 1054, found enhanced in the 30S subunit, remains high in the complete ribosome. Obviously, important conformational rearrangements occur in this region upon assembly and probably upon subunit association, and the observed protection may well result from a conformational adjustment.

Two three-dimensional models of 16S rRNA have recently been proposed, one by the group of Brimacombe (Brimacombe et al., 1988) and, after completion of this study, one by the group of Noller (Stern et al., 1988c). The two models present a certain degree of agreement, but extensive discrepencies are also noted. The Cartesian coordinate system given for the model of Brimacombe et al. (1988, Table III) greatly facilitates comparison with our data. The helices have been numbered in Figure 3 according to these authors to make comparison easy. We find a general satisfying agreement between our results and the model of Brimacombe's group. It turns out that a large majority of phosphates found protected from ENU by the 50S subunit are in or near helices having a negative coordinate value along the z axis (from −49 Å for helix 45 to 0 for helix 22), according to the coordinates system. These RNA regions are also located on the same face of the model. In particular, the strong protections observed in the 3′-terminal region and the central domain correlate with their high negative values (helix 45 = −49, helix 24 = −44, helix 27 = −39, helix 26a = −35), suggesting that these regions are in close contact with the large subunit. The two major exceptions concern helices 32 and 34 for which a positive value is given (+27 and +21, respectively). The protections observed in these helices are not explained by the model of Stern et al. either, since these helices are clearly located on the solvent side. As already discussed previously, conformational rearrangements have been evidenced in this region that might account for the observed protections. Some of the protected regions have a low negative coordinate value (helix 22 = 0, helices 38 and 11 = −4, helix 35 = −6, helix 39 = −7, helix 23 = −8, helix 28 = −9, helix 26 = −10), suggesting that they are positioned rather deep in the subunit. The protection in this case is most likely the consequence of a polyspecific effect involving shielding by both proteins and the 50S subunit. On the other hand, several helices have a negative coordinate value but are not found protected (helix 3 = −12, helix 16 = −17, helix 17 = −6, helix 20 = −28, helix 43 = −2). In the Berlin model, helices 3, 16, and 17 are located on the edge of the body of the subunit, opposite to the platform (containing helices 45 and 24), suggesting that this part of the subunit is not shielded by the 50S particle. The absence of protection of helix 20 is more difficult to fit with this model. One major discrepancy between the two models is the location of helices in the 565–610 region of the central domain on the solvent side in the model of Noller's group, while they are placed at the 50S interface by Brimacombe's group. Therefore, the lack of protection of helix 20 would be rather consistent with its orientation on the solvent side. Conversely, helices 13 and 14 which are not found protected from ENU have been placed by Noller's group at the interface and by Brimacombe's group on the solvent side. Note that several isolated protections and reinforced protections are observed in helices 4 (=0), 5 (=28), and 44 (=14), which can be interpreted as the result of some allosteric adjustment rather than proper shielding effect. The 50S association also induces enhanced reactivities which are clustered in the central domain (nucleotides 819–838), in this particular region postulated to bind initiation factor III and to undergo a conformational switch upon binding of this factor

(Ehresmann et al., 1986). Interestingly, ENU alkylation allows one to reveal dynamic properties in this region and conformational adjustments induced by both assembly and association processes. It might be relevant that a pseudoknot-type structure has recently been postulated in this region (Stern et al., 1988c). Enhanced stops of elongation, interpreted as increased spontaneous cleavages, are also induced (at positions 80–81, 355, 840–841, 1423, 1531, and 1535), revealing an increased flexibility in these regions. It must be mentioned that allosteric transitions induced by the binding of the large subunit in the 3′-terminal domain of 16S rRNA have also been evidenced using lead(II)-induced cleavage as a probe (Gornicki et al., 1989).

In conclusion, probing 16S rRNA with ENU has allowed us to get precise information at the atomic level and to provide evidence for conformational adjustments induced by subunit assembly and ribosome association. Compared to other chemical probes, ENU has the advantage of attacking without any discrimination against single-stranded and double-stranded regions. This reagent permits us to probe the phosphate backbone of the RNA whereas other chemical probes test base positions. Therefore, the information provided by ENU probing is different and complementary to other data. This work allows us to get new information on the tertiary structure of the RNA and specific information on the orientation of helices and loops in the subunit relative to the proteins and to the subunit interface. The present data will be, with others, helpful in any attempt of modeling or refinement of models.

ACKNOWLEDGMENTS

We are indebted to J. Colin for the synthesis of the deoxyribooligonucleotides.

REFERENCES

Baudin, F., Ehresmann, C., Romby, P., Mougel, M., Colin, J., Lempereur, L., Bachellerie, J. P., Ebel, J. P., & Ehresmann, B. (1987) *Biochimie 69*, 1081–1096.

Brimacombe, R., Atmadja, J., Stiege, W., & Schüler, D. (1988) *J. Mol. Biol. 199*, 115–136.

Capel, M. S., Engelmann, D. M., Freeborn, B. R., Kjeldgaard, M., Langer, J. A., Ramakrishnan, V., Schindler, D. G., Schneider, D. K., Scoenborn, B. P., Sillers, I. Y., Yabuki, S., & Moore, P. B. (1987) *Science 238*, 1171–1185.

Chapman, N. M., & Noller, H. F. (1977) *J. Mol.* Biol. *109*, 131–149.

Chiaruttini, C., Expert-Bezançon, A., Hayes, D., & Ehresmann, B. (1982) *Nucleic Acids Res. 10*, 7657–7676.

Chiaruttini, C., Milet, M., Hayes, D., & Expert-Bezançon, A. (1986) *Eur. J. Biochem. 160*, 363–370.

Dock-Bregeon, A. C., & Moras, D. (1987) *Cold Spring Harbor Symp. Quant. Biol. 52*, 113–121.

Douthwaite, S., Christensen, A., & Garrett, R. A. (1983) *J. Mol. Biol. 169*, 249–279.

Ehresmann, B., Backendorf, C., Ehresmann, C., Millon, R., & Ebel, J. P. (1980) *Eur. J. Biochem. 109*, 255–262.

Ehresmann, C., Moine, H., Mougel, M., Dondon, J., Grunberg-Manago, M., Ebel, J. P., & Ehresmann, B. (1986) *Nucleic Acids Res. 14*, 4803–4821.

Ehresmann, C., Baudin, F., Mougel, M., Romby, P., Ebel, J. P., & Ehresmann, B. (1987) *Nucleic Acids Res. 15*, 9109–9128.

England, T. E., & Uhlenbeck, O. C. (1978) *Nature 275*, 560–561.

Expert-Bezançon, A., & Wollenzien, P. L. (1985) *J. Mol. Biol. 184*, 53–66.

Florentz, C., & Giegé, R. (1986) *J. Mol. Biol. 191*, 117–130.

Florentz, C., Briand, J. P., Romby, P., Hirth, L., Ebel, J. P., & Giegé, R. (1982) *EMBO J. 1*, 269–276.

Garret, M., Labouesse, B., Litvak, S., Romby, P., Ebel, J. P., & Giegé, R. (1984a) *Eur. J. Biochem. 138*, 67–75.

Garret, M., Romby, P., Giegé, R., & Litvak, S. (1984b) *Nucleic Acids Res. 12*, 2259–2271.

Golinska, B., Millon, R., Backendorf, C., Olomucki, M., Ebel, J. P., & Ehresmann, B. (1981) *Eur. J. Biochem. 115*, 479–484.

Gorniski, P., Baudin, F., Romby, P., Wiewiorowski, M., Kryzosiak, W., Ebel, J. P., Ehresmann, C., & Ehresmann, B. (1989) *J. Biomol. Struct. Dyn. 6*, 971–984.

Greuer, B., Osswald, M., Brimacombe, R., & Stöffler, G. (1987) *Nucleic Acids Res. 15*, 3241–3255.

Herr, W., Chapman, N. M., & Noller, H. F. (1979) *J. Mol. Biol. 130*, 433–449.

Holbrook, S. R., Sussman, J. L., Warrant, R. W., & Kim, S. H. (1978) *J. Mol. Biol. 123*, 631–660.

Jack, A., Ladner, J. E., Rhodes, D., Brown, R. S., & Klug, A. (1977) *J. Mol. Biol. 111*, 619–649.

Lavery, R., & Pullman, A. (1984) *Biophys. Chem. 19*, 171–181.

McDougall, J., & Nazar, R. N. (1986) *Nucleic Acids Res. 15*, 161–179.

Moazed, D., & Noller, H. F. (1987) *Nature 327*, 389–394.

Moazed, D., Stern, S., & Noller, H. F. (1986) *J. Mol. Biol. 187*, 399–416.

Moine, H., Bienaimé, C., Mougel, M., Reinbolt, J., Ebel, J. P., Ehresmann, C., & Ehresmann, B. (1988) *FEBS Lett. 228*, 1–6.

Mougel, M., Eyermann, F., Westhof, E., Romby, P., Expert-Bezançon, A., Ebel, J. P., Ehresmann, B., & Ehresmann, C. (1987) *J. Mol. Biol. 198*, 91–107.

Mougel, M., Philippe, C., Ebel, J. P., Ehresmann, B., & Ehresmann, C. (1988) *Nucleic Acids Res. 7*, 2825–2839.

Ofengand, J., Ciesolka, J., Denman, R., & Nurse, K. (1986) in *Structure, Function and Genetics of Ribosomes* (Hardesty, B., & Kramer, G., Eds.) pp 473–494, Springer-Verlag, Berlin.

Powers, T., Changchien, L. M., Craven, G. R., & Noller, H. F. (1988a) *J. Mol. Biol. 200*, 309–319.

Powers, T., Stern, S., Changchien, L. M., & Noller, H. F. (1988b) *J. Mol. Biol. 201*, 601–716.

Quigley, G. J., Teeter, M. M., & Rich, A. (1978) *Proc. Natl. Acad. Sci. U.S.A. 75*, 64–68.

Riehl, N., Giegé, R., Ebel, J. P., & Ehresmann, B. (1983) *FEBS Lett. 154*, 42–46.

Romaniuk, P. J., Leal de Stevenson, I., Ehresmann, C., Romby, P., & Ehresmann, B. (1988) *Nucleic Acids Res. 16*, 2295–2312.

Romby, P., Moras, D., Bergdoll, M., Dumas, P., Vlassov, V. V., Westhof, E., Ebel, J. P., & Giegé, R. (1985) *J. Mol. Biol. 184*, 455–471.

Romby, P., Carbon, P., Westhof, E., Ehresmann, C., Ebel, J. P., Ehresmann, B., & Giegé, R. (1987) *J. Biomol. Struct. Dyn. 5*, 669–687.

Romby, P., Westhof, E., Toukifimpa, R., Mache, R., Ebel, J. P., Ehresmann, C., & Ehresmann, B. (1988) *Biochemistry 27*, 4721–4730.

Sanger, F., Nicklen, S., & Coulson, A. R. (1977) *Proc. Natl. Acad. Sci. U.S.A. 74*, 5463–5467.

Sigmund, C., Ettayebi, M., & Morgan, E. (1984) *Nucleic Acids Res. 12*, 4653–4663.

Silberklang, M., Gillam, A. M., & RajBhandary, U. L. (1977) *Nucleic Acids Res. 4*, 4091–4108.
Stern, S., Wilson, R. C., & Noller, H. F. (1986) *J. Mol. Biol. 192*, 101–110.
Stern, S., Changchien, L. M., Craven, G. R., & Noller, H. F. (1988a) *J. Mol. Biol. 200*, 291–299.
Stern, S., Powers, T., Changchien, L. M., & Noller, H. F. (1988b) *J. Mol. Biol. 201*, 683–695.
Stern, S., Weiser, B., & Noller, H. F. (1988c) *J. Mol. Biol. 204*, 447–481.
Svensson, P., Changchien, L. M., Craven, G. R., & Noller, H. F. (1988) *J. Mol. Biol. 200*, 301–308.
Thompson, J. F., & Hearst, J. E. (1983) *Cell 32*, 1355–1365.
Vassilenko, S. K., Carbon, P., Ebel, J. P., & Ehresmann, C. (1981) *J. Mol. Biol. 152*, 699–721.
Vlassov, V. V., Giegé, R., & Ebel, J. P. (1981) *Eur. J. Biochem. 119*, 51–59.
Vlassov, V. V., Kern, D., Romby, P., Giegé, R., & Ebel, J. P. (1983) *Eur. J. Biochem. 132*, 537–544.
Westhof, E., Dumas, P., & Moras, D. (1985) *J. Mol. Biol. 184*, 119–145.

Mechanism of Polynucleotide Phosphorylase†

Michael Sulewski,‡ Silvio P. Marchese-Ragona,§ Kenneth A. Johnson,§ and Stephen J. Benkovic*,‡
Department of Chemistry and Department of Molecular and Cell Biology, The Pennsylvania State University, University Park, Pennsylvania 16802
Received November 14, 1988

ABSTRACT: The de novo polymerization of RNA initiated by polynucleotide phosphorylase from nucleoside diphosphates was examined. End group analysis performed under conditions designed to specifically end label the polymer revealed no evidence for a 5′-pyrophosphate-terminated polymer. However, we observed preferential incorporation of the ADPαS(R_P) diastereomer into the 5′ end (Marlier & Benkovic, 1982) in chain initiation, suggesting that the enzyme incorporates a nucleoside diphosphate specifically into the 5′ end of the product, with subsequent enzymatic removal of the polyphosphate linkage. No evidence could be obtained for a covalent adduct between the enzyme and the 5′ end of the polymer chain, despite the high processivity of the polymerization reaction. Gel electrophoretic analysis showed the polymer to be highly disperse, varying from 1 to 30 kb. Scanning transmission electron microscopy supported this product analysis and further suggested that (i) each subunit can produce an RNA polymer and (ii) both 5′ and 3′ ends of the RNA can be bound simultaneously to the same or differing enzyme molecules.

The primer-independent form of polynucleotide phosphorylase (PNPase)[1] from *Micrococcus leuteus* catalyzes the reversible polymerization of nucleoside diphosphates to polyribonucleotides and inorganic phosphate. These polynucleotides are synthesized de novo in the 5′ → 3′ direction, resulting in high molecular weight polymers (Godefroy-Colburn & Grunberg-Manago, 1972). Polymerization by form I enzyme is stimulated only slightly by oligonucleotides (Moses & Singer, 1970). Since its discovery by Grunberg-Manago and Ochoa (1955), PNPase has been studied in great detail as a tool for the synthesis of model nucleic acids (Engel & Davidson, 1978; Mackey & Gilham, 1971; Littauer & Soreq, 1982). However, the elementary steps in the de novo initiation mechanism have not been established and a well-defined biological function has remained elusive.

Recently, the first purification of the form I PNPase from *M. luteus* free of contaminating activities was reported (Barbehenn et al., 1982). The availability of contaminant-free PNPase has made possible the first unambiguous determination of several aspects of the de novo polymerization mechanism (Harvey & Grunberg-Manago, 1970; Marlier & Benkovic, 1982). The earlier report of Barbehenn indicated that a homogeneous population of polymeric products was formed, apparently by a highly processive mechanism (Barbehenn et al., 1982). Data bearing on the nature and origin of the 5′ end group of the polymeric products will be presented in this paper. In addition, experiments utilizing rapid quench techniques and scanning transmission electron microscopy were performed to quantitate the degree of processivity and the distribution of products formed, leading us to suggest an unusual mechanism of de novo polymerization.

Experimental Procedures

Materials. Polynucleotide phosphorylase (PNPase) was obtained from Dr. Claude Klee (NIH) or purified from *M. luteus* cells (ATCC 4698). The *M. luteus* cells were grown

† This work was supported by NIH Grant GM13306 to S.J.B. and in part by NIH Grant GM26726 to K.A.J. K.A.J. was supported by an Established Investigatorship from the American Heart Association with funds contributed in part by the Pennsylvania Affiliate.
* Author to whom correspondence should be addressed.
‡ Department of Chemistry.
§ Department of Molecular and Cell Biology.

[1] Abbreviations: AMPS, adenosine 5′-*O*-(thiophosphate); ADPαS(R_P) and ADPαS(S_P), diastereomers of adenosine 5′-*O*-(1-thiodiphosphate); ApA, adenylyl(3′–5′)adenosine; HEPES, *N*-(2-hydroxyethyl)piperazine-*N*′-2-ethanesulfonic acid; MOPS, 3-(*N*-morpholino)-propanesulfonic acid; pApA, 5′-phosphoadenylyl(3′–5′)adenosine; PNPase (form I), polynucleotide phosphorylase, primer-independent form; PNPase (form T), polynucleotide phosphorylase, primer-dependent form; poly(A), poly(adenylic acid); poly(I), poly(inosinic acid); poly(U), poly(uridylic acid); poly(N)$_{ox}$, any polyribonucleotide with both a 5′- and a 3′-phosphate; ppApA, 5′-diphosphoadenylyl(3′–5′)adenosine; p(S)Ap(S), adenosine 5′,3′-bis(thiophosphate); p(S)Ap(O), adenosine 5′-(thiophosphate) 3′-phosphate; pp(S)Ap(S), adenosine 5′-*O*-(1-thiodiphosphate) 3′-*O*-(thiophosphate); STEM, scanning transmission electron microscopy; TEAB, triethylammonium bicarbonate; Tris, tris(hydroxymethyl)aminomethane.

0006-2960/89/0428-5855$01.50/0